
ANOTHER LOOK AT SYNTHETIC-TYPE CONTROL CHARTS

A PREPRINT

✉ **Sven Knoth**

Dep. of Mathematics & Statistics
 Helmut Schmidt University
 Hamburg, Germany
 knoth@hsu-hh.de

November 05, 2021

Abstract

During the last two decades, in statistical process monitoring plentiful new methods appeared with synthetic-type control charts being a prominent constituent. These charts became popular designs for several reasons. The two most important ones are simplicity and proclaimed excellent change point detection performance. Whereas there is no doubt about the former, we deal here with the latter. We will demonstrate that their performance is questionable. Expanding on some previous skeptical articles we want to critically reflect upon recently developed variants of synthetic-type charts in order to emphasize that there is little reason to apply and to push this special class of control charts.

Keywords average run-length · conditional expected delay · control chart · statistical process monitoring · steady-state

1 Introduction

From the statistical tools, we know as control charts, the majority was created in the 20th century. During the last years, however, numerous new concepts were introduced. The synthetic chart, proposed by [Wu and Spedding \(2000b,a\)](#), is a special example. On the one hand, it fascinates with its simple design and its explicit solutions of the Average Run Length (ARL) equation and related measures. The ARL is the expected number of samples or individual observations until the control chart declares that a change happened alias lack of control was detected ([Shewhart, 1925](#)). It comes in various types, where the most popular ones are the zero-state and steady-state ARL ([Crosier, 1986](#)). And on the other hand, in [Wu and Spedding \(2000b\)](#) the synthetic chart was proclaimed as superior in terms of the zero-state ARL, (unintentionally) concealing that it was equipped with a solid head-start. So [Davis and Woodall \(2002\)](#) criticized this pattern and suggested two key elements: Enforce the steady-state ARL as performance measure which captures potentially misleading side effects of introducing head-starts. Second, endow the older runs rule chart, which differentiates between the change directions (called side-sensitive), as well with a head-start. This rather cautious critique did not block the further development of synthetic charts. Instead, these charts became really popular. The more recent [Knoth \(2016\)](#) was already much more explicit in its criticism. Nevertheless, synthetic charts remained highly attractive. In particular, [Rakitzis et al. \(2019\)](#) claimed that [Knoth \(2016\)](#) did consider only the original synthetic chart of [Wu and Spedding \(2000b\)](#). This is partially correct, but the general message would be the same anyway: Synthetic charts and all their derivatives (published so far) are clearly dominated by older control charts. For example, two of the four synthetic-type charts in [Chakraborti and Rakitzis \(2021\)](#), namely both standalone ones, were analyzed in [Knoth \(2016\)](#). Here, we will utilize Exponentially Weighted Moving Average (EWMA) charts, which will be compared to all four plain synthetic-type charts. For the sake of a concise presentation, we touch only briefly combinations of synthetic with Shewhart-type charts, which were called improved synthetic charts in [Rakitzis et al. \(2019\)](#). Their “natural” counterpart is a Shewhart-EWMA combo ([Lucas and Saccucci, 1990](#); [Capizzi and Masarotto, 2010](#)). Thus, we provide a

thorough ARL (zero- and steady-state) analysis of 8 (including charts without head-start like Shongwe and Graham, 2018) different synthetic-type charts and EWMA charts.

In Section 2 we describe all considered control charts in more detail. Later, in Section 3 we elaborate upon the steady-state ARL concept, where some confusions have to be clarified. Our main results appear in Section 4, where we compare all the charts by looking at the zero-state ARL, conditional expected delay (CED) and the steady-state ARL. Finally, we assemble our conclusions in Section 5. In the Appendix some side results are given.

2 Classification scheme of synthetic-type charts

As Rakitzis et al. (2019) and others mentioned, the constitutive element of a synthetic chart is that two warnings or signals are needed to trigger the actual alarm. And these two signals should not be too “*far away from each other*”. Thus, synthetic charts are special runs (or scan) rules charts, because they could be expressed as 2-of- $H+1$ runs rules, with $H \in \{1, 2, \dots\}$, cf. to Davis and Woodall (2002); Bersimis et al. (2020). Differently to Rakitzis et al. (2019), we consider not only the head-start versions. Instead, following Shongwe and Graham (2018, 2019) and Bersimis et al. (2020), we investigate common and head-start synthetic-type charts. In the here following Table 1, we list the 8 synthetic-type charts with their initial reference.

Table 1: Simplified version of Table 1 in Shongwe and Graham (2018), i. e. only 2-of- $H+1$ designs.

#	label	w/o head-start		w/ head-start	
1	“true” synthetic	R_1	Derman and Ross (1997) ¹	S_1	Wu and Spedding (2000b)
2	side-sensitive	R_2	Klein (2000)	S_2	Davis and Woodall (2002)
3	revised	R_3	Machado and Costa (2014) ²	S_3	Shongwe and Graham (2018)
4	modified	R_4	Antzoulakos and Rakitzis (2008)	S_4	Shongwe and Graham (2018)

Besides Table 1, which is a simplified and reduced version of Table 1 in Shongwe and Graham (2018), we want to provide some more constructional details. For simplicity, we assume individual normally distributed observations with mean μ and standard deviation σ (more details in the next section). We set exemplary $H = 3$. Between two signals alias two observations beyond the limits, there must be at most two “unobtrusive” observations to trigger an alarm. For “true” synthetic charts (in the narrower sense), it is not important whether the two signals are raised on the same side of the chart, whereas the remaining three designs require the same side. In Figure 1, we plotted the center line at the in-control mean μ_0 and two limits at $\mu_0 \pm k\sigma_0$. Here, σ_0 denotes the in-control standard deviation which is assumed to be constant and known. The design

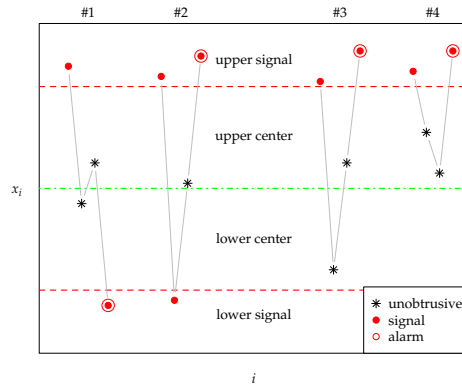


Figure 1: Four observations that form an alarm pattern for four different synthetic-type charts with $H = 3$.

¹Derman and Ross (1997): “Probably the easiest way to construct a control chart that considers each subgroup average in relation to those around it is to define a chart that declares a process out of control if two successive averages differ from μ by more than $c\sigma$ for some value c .”

²Machado and Costa (2014): “The transient states describe the position of the last L sample points; ‘1’ means that the sample point fell below the LCL, ‘0’ means that the sample point fell in the central region, and ‘1’ means that the sample point fell above the UCL.”

parameter k controls the detection behavior and is typically chosen to achieve a pre-defined in-control ARL. Pattern #1 in Figure 1 would trigger an alarm only for chart #1. The next pattern raises an alarm for the common 2-of-4 runs rule, where the lower signal has no impact to the final alarm. Chart #3 requests that the observations enclosed by the two upper signals reside between the limits. Later we will see that there are no big performance differences between these two chart designs. The most involved design is #4, where the in-between observations have to be on the same side like the signaling points. The patterns are chosen so that pattern #4 flags an alarm for all four charts, whereas pattern #3 does it only for #1, #2 and #3, etc. Of course, these different patterns demand distinct values of k , namely $2.2087 > 2.0760 > 2.0723 > 1.9642$ for #1, ..., #4, respectively, for $H = 3$ and in-control ARL 500. Note that the values for charts with head-start are slightly larger. After explaining the differences between the rows in Table 1, we want to describe the disparity between the columns. Thus, it is about head-start and no head-start. The former presumes that the last data point, just before monitoring was started, would trigger a signal. Hence, we need only one further signal to raise an alarm. Except for #1, however, we have to know whether the signal was above the upper or below the lower limit. This problem is dealt with pragmatically, that is, given the first observed signal, we just imply that the hidden signal was on the same side, providing kind of a wildcard head-start³. There are some side effects to the Markov chain modeling, except for #1, of course. Specifically, we have to introduce further states of the chain that are related to this particular starting behavior. In Table 2, we indicate the resulting number of transient states we obtain for the underlying Markov chain model, cf. to Shongwe and Graham (2018). We added as well the chart labels used in Shongwe and Graham (2018) and Bersimis et al. (2020). The smallest value, $H + 1$, is known from Davis and Woodall (2002). The latter reported as well

Table 2: Number of transient states, 2-of- $H + 1$ rules, see Table 1.

#	w/o head-start		w/ head-start	
1	DR:	$H + 1$	WS:	$H + 1$
2	KL:	$H^2 + H + 1$	DW:	$H^2 + 2H + 1$
3	MC1:	$2H + 1$	MC2:	$3H + 1$
4	AR:	$2H + 1$	MSS:	$4H$

the largest value in Table 2, observed for the DW chart, namely $(H + 1)^2$. From the latter size, one can straightforwardly derive the number for the general KL chart, that is, $H^2 + H + 1$ (Knoth, 2016, dealt with three synthetic-type charts: WS, KL and DW). The dimension $2H + 1$ was given in Machado and Costa (2014). The remaining numbers could be found in Shongwe and Graham (2018).

Before continuing with the competitor EWMA, we want to mention that the very recent Chakraborti and Rakitzis (2021) labeled the synthetic-type charts differently. Their S_1 and S_3 correspond to WS (our S_1) and DW (our S_2), respectively. The remaining two in Chakraborti and Rakitzis (2021), S_2 and S_4 , are just the latter combined with a Shewhart alarm rule.

As already mentioned, we utilize the common EWMA (Roberts, 1959) chart with varying limits as the main competitor to all the synthetic-type charts. Picking an appropriate value for the smoothing constant $0 < \lambda \leq 1$ (we favor here 0.25 and 0.1), we create the following sequence of EWMA statistics (Lucas and Saccucci, 1990; Montgomery, 2019):

$$Z_0 = \mu_0 \quad , \quad Z_i = (1 - \lambda)Z_{i-1} + \lambda X_i \quad , \quad i = 1, 2, \dots, \quad (1)$$

$$L_E = \min \left\{ i \geq 1 : |Z_i - \mu_0| > c_E \sqrt{(1 - (1 - \lambda)^{2i}) \frac{\lambda}{2 - \lambda} \sigma_0^2} \right\}. \quad (2)$$

Besides the series $\{Z_i\}$ we get the run-length alias stopping time L_E which simply counts the number of observations until the first alarm. Fortunately, there are numerical routines (Crowder, 1987; Knoth, 2003, 2005) for calculating all the measures we deploy in this contribution (see next section). Of course, the results are only approximations (differently to the synthetic-type charts, where the corresponding Markov chains are exact models), the accuracy of the said numerical procedures is sufficiently high. Eventually we want to note that we apply their implementations in the R package `spc` (Knoth, 2021a).

³Davis and Woodall (2002): “The initial state is $0 \pm$; that is, the most recent observation at the onset of monitoring is considered to be beyond control limits on both sides of the center line.”

3 Steady-state ARL and other measures

As told in the previous section, we consider an independent series X_1, X_2, \dots following a normal distribution with mean μ and standard deviation σ . To incorporate a potential change, we apply the change point (τ) model

$$\mu = \begin{cases} \mu_0 = 0 & , t < \tau \\ \mu_1 = \delta & , t \geq \tau \end{cases} . \quad (3)$$

Regarding the standard deviation (variance) we make the common assumption that it is known, $\sigma = \sigma_0 = 1$ (otherwise normalize the X_t), and it remains constant.

With L we denote the run length (stopping time), which is the number of observed X_i values until an alarm is raised. The expected values of L for the two situations $\tau = 1$ and $\tau = \infty$ constitute the well-known zero-state Average Run Length (ARL), cf. to [Page \(1954\)](#); [Crosier \(1986\)](#). Mostly, the control charts are setup to yield a pre-defined in-control ARL, i. e. $E_\infty(L) = A$ for some suitably large number A (here we set $A = 500$). For a given control chart design, it is a common task to determine out-of-control ARL values, $E_1(L)$, for specified values of δ . The resulting ARL profiles are typically used to judge the detection performance over a range of changes δ and to compare charts to each other.

Besides the simple case $\tau = 1$ in (3), we determine the series of conditional expected delays (CED)

$$D_\tau = E_\tau(L - \tau + 1 \mid L \geq \tau) \quad , \quad \tau = 1, 2, \dots$$

and its limit, the conditional steady-state ARL

$$\mathcal{D}_1 = \lim_{\tau \rightarrow \infty} D_\tau .$$

Both $\{D_\tau\}$ and \mathcal{D}_1 are functions of δ . For all charts considered here (EWMA and synthetic-type), the series $\{D_\tau\}$ converges quickly to \mathcal{D}_1 . Besides \mathcal{D}_1 , one can utilize the cyclical steady-state ARL \mathcal{D}_2 , which incorporates re-starts after getting a false alarm. See [Taylor \(1968\)](#), [Crosier \(1986\)](#) and the recent [Knoth \(2021b\)](#) for more details. It is defined as follows:

$$\mathcal{D}_2 := \lim_{\tau \rightarrow \infty} E_\tau(L_\star - \tau + 1)$$

with $L_\star = L_1 + L_2 + \dots + L_{I_\tau-1} + L_{I_\tau}$ and $I_\tau = \min \left\{ i \geq 1 : \sum_{j=1}^i L_j \geq \tau \right\} .$

Thus, after some number of false alarms ($L_1, L_2, \dots, L_{I_\tau-1}$ as number of observations to the next false alarm) the first true alarm appears at observation $L_\star \geq \tau$. The term $L_\star - \tau + 1$ denotes the resulting detection delay. Of course, the restarting pattern (for EWMA typically at μ_0 , whereas for the synthetic-type charts various ideas were investigated) influences the actual value of \mathcal{D}_2 .

By denoting \mathbb{Q} the transition matrix of transient states, \mathbb{I} the identity matrix and $\mathbf{1}$ a vector of ones, we start with the classical ARL (vector ℓ) result of [Brook and Evans \(1972\)](#)

$$\ell = (\mathbb{I} - \mathbb{Q})^{-1} \mathbf{1} ,$$

and continue with some prerequisites for the steady-state vectors ([Knoth, 2021b](#)):

$$\begin{aligned} \varrho \psi_1 &= \mathbb{Q}' \psi_1 && \text{--- left eigenvector of the dominant eigenvalue } \varrho , \\ \psi_2 &= (\mathbb{I} - \mathbb{Q}')^{-1} \mathbf{e}_1 && \text{--- } \mathbf{e}_1 \text{ consists of zeros except for the restart state, where a 1 is set .} \end{aligned}$$

The equation for ψ_1 was given in [Brook and Evans \(1972\)](#), whereas the ψ_2 equation was included in [Darroch and Seneta \(1965\)](#). Both vectors will be normalized (i. e. $\mathbf{1}' \psi_i = 1$, $i = 1, 2$). Then the two steady-state ARLs are calculated via $\mathcal{D}_i = \psi_i' \ell$, $i = 1, 2$ (exact for synthetic-type, approximation for EWMA). For the true synthetic chart ([Wu and Spedding, 2000b](#)), the following explicit solutions were derived ([Knoth, 2016](#)),

$\Phi(\cdot)$ denoting the cdf of the standard normal distribution:

$$\begin{aligned}
 p &= p(k; \delta) = 1 - [\Phi(k - \delta) - \Phi(-k - \delta)] \quad , \quad q = 1 - p \quad , \quad r = p(1 - q^H), \\
 \ell' &= \begin{pmatrix} 0 & 1 & \dots & H-1 & H \\ \frac{1}{r} & \frac{1+q^H(q^{-1}-1)}{r} & \dots & \frac{1+q^H(q^{-(H-1)}-1)}{r} & \frac{1}{r} + \frac{1}{p} \end{pmatrix}, \\
 \psi'_1 &= \begin{pmatrix} 0 & 1 & \dots & H-1 & H \\ s & \frac{q}{\varrho}s & \dots & \left(\frac{q}{\varrho}\right)^{H-1}s & \frac{\varrho}{p}s \end{pmatrix} \quad , \quad s = 1 - q/\varrho, \\
 \psi'_2 &= \begin{pmatrix} 0 & 1 & \dots & H-1 & H \\ p & pq & \dots & pq^{H-1} & q^H \end{pmatrix}.
 \end{aligned} \tag{4}$$

Recall that the restart for ψ_2 happens at state 0, which refers to the solid head-start situation. Note that [Wu et al. \(2010\)](#) utilized the same restart state. However, [Shongwe and Graham \(2019\)](#) considered a different restart state, namely H that corresponds to the no head-start case. The resulting vector is

$$\psi'_3 = \frac{1}{2 - q^H} \begin{pmatrix} 0 & 1 & \dots & H-1 & H \\ p & pq & \dots & pq^{H-1} & 1 \end{pmatrix}.$$

The vectors ψ_2 and ψ_3 differ in the entry for state H , namely q^H and 1, respectively, and in the normalizing constant, 1 and $1/(2 - q^H)$, respectively. The impact to the resulting \mathcal{D}_2 is not substantial. [Shongwe and Graham \(2019\)](#) did not explain why they used a different head-start. Moreover, it remains as well unclear, why they proposed two ways of calculating the cyclical steady-state vector. First, there are more than two approaches. Second, all these different procedures provide equal solutions (except for the scaling constant). For an elaborated discussion refer to [Knoth \(2021b\)](#). A more important problem, however, is the wrong result of both [Shongwe and Graham \(2019, p.192 and 195\)](#) and already [Machado and Costa \(2014, p.2899\)](#) for \mathcal{D}_1 (conditional), in particular for its steady-state vector (ψ_1). By following the erroneous path in [Crosier \(1986\)](#), they obtained:

$$\psi'_4 = \frac{1}{1 + Hp} \begin{pmatrix} 0 & 1 & \dots & H-1 & H \\ p & p & \dots & p & 1 \end{pmatrix}.$$

First, recall that [Crosier \(1986\)](#) introduced the terms conditional and cyclical, while he also provided Markov chain algorithms to calculate these steady-state ARLs. His procedure for the cyclical steady-state ARL is correct, despite it is not the one indicated in [Shongwe and Graham \(2019, p.191\)](#). However, the approach to get the conditional steady-state ARL by following “the matrix $\mathbb{R} \dots$ can be scaled up so that each row of the matrix sums to 1” ([Crosier, 1986, p.193](#)) is wrong. For more details we refer to [Knoth \(2021b\)](#). The surprisingly simple ψ_4 is the output of this wrong algorithm applied to the synthetic (in the narrower sense) chart. We wonder why none of the above authors questioned this nearly uniform distribution. The good news are that the numerical differences when using ψ_1, \dots, ψ_4 are not large, see Appendix [A.1](#). Therefore it is not too restrictive to apply the conditional steady-state ARL \mathcal{D}_1 relying on ψ_1 and the related CED \mathcal{D}_τ for the rest of the paper. Note that neither in [Rakitzis et al. \(2019, p.5\)](#) nor in [Chakraborti and Rakitzis \(2021, p.13\)](#) the discussion of the steady-state ARL did touch these subtle complications.

4 Comparison study

We start with a CED analysis of the four synthetic-type charts with head-start. All considered control charts are designed to have an in-control ARL, $E_\infty(L)$, of 500. For the aforementioned charts, labeled as S_1, \dots, S_4 , we determine the CED \mathcal{D}_τ for $\tau = 1, 2, \dots, 50$. Moreover, we plot the CED profiles for $H = 1, 2, \dots, 25$. In Figure [2](#) we display besides the 25 mentioned profiles two EWMA ($\lambda = 0.25$ and $= 0.1$) CED profiles.

First, we observe that the detection performance gets better along S_1, \dots, S_4 . Second, there is a pronounced difference between S_4 and the other synthetic-type charts. For the latter, there is a clearly identifiable CED maximum at $\tau = H + 1$. Later we will learn about the root cause of this behavior (see Figure [7](#)). The larger H , the sharper is the increase from $\tau = 1$ to $\tau = H + 1$. In case of S_4 for all $H = 1, \dots, 25$, stability of the \mathcal{D}_τ is reached before $\tau = 10$. However, the S_4 profiles are only a smoothed version of the other much more pronounced ones. Looking at the actual numbers, we receive the same $\tau = H + 1$ as argument of the maximum. Nonetheless, the S_4 version could be sufficiently well characterized by the zero-state and the steady-state ARL, whereas for the others the inner maximum is important too, because it is considerably larger than the

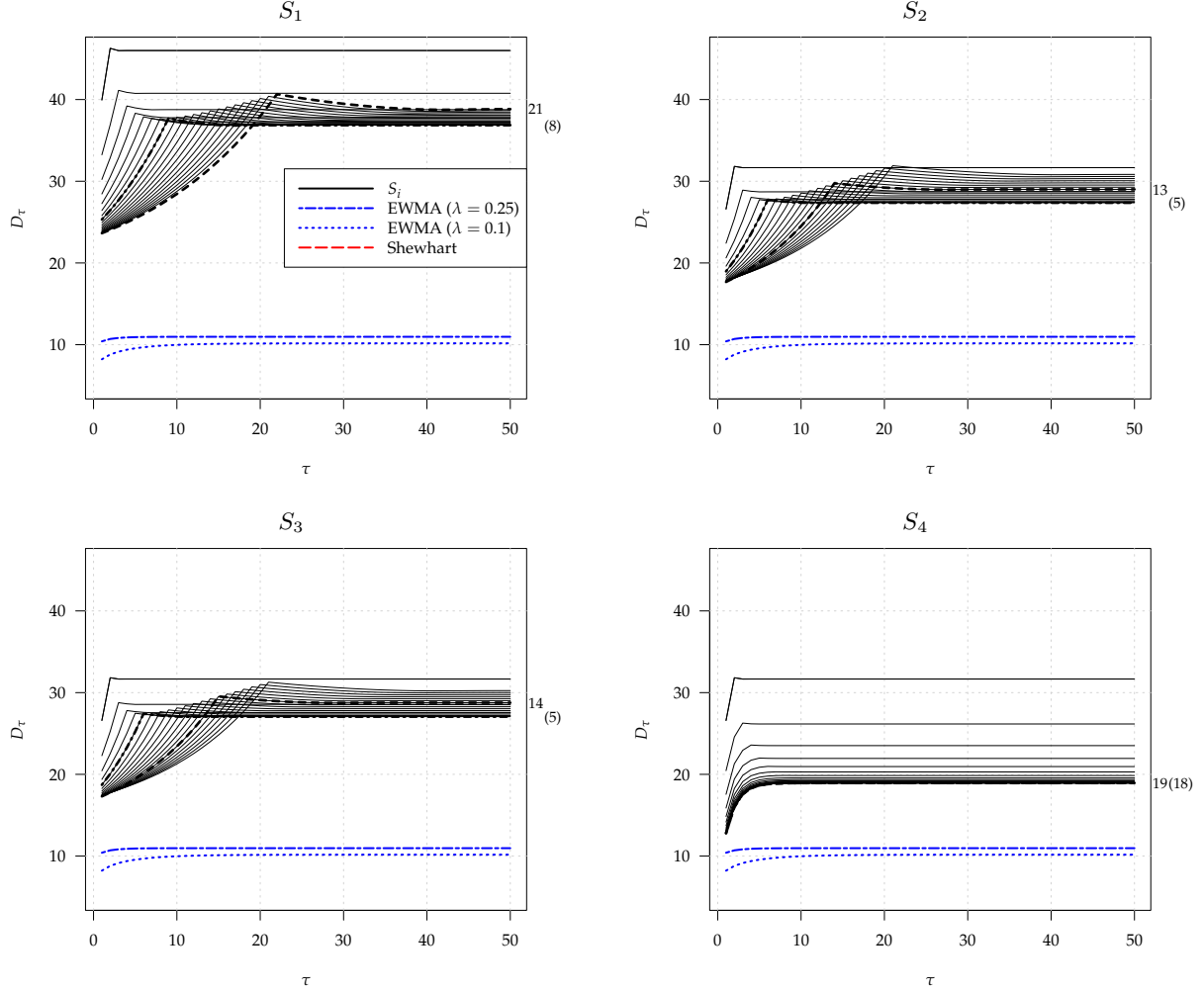


Figure 2: D_τ profiles for four synthetic-type charts with head-start, $H = 1, 2, \dots, 25$, best scheme (zero-state and steady-state) bold (dashed and dash-dotted) lines, shift $\delta = 1$, two EWMA charts; in-control ARL 500.

other two measures. In Figure 2, we marked the profiles with the lowest zero-state and steady-state ARL, by bold dashed and dash-dotted lines, respectively, and annotated the related H value on the right-hand margin. The H for the minimum zero-state ARL ($H = 21, 13, 14$) is substantially larger than for the steady-state one ($H = 8, 5, 5$), except for S_4 (values are quite similar: $H = 19$ and 18). For all synthetic charts with head-start, the zero-state ARL is markedly smaller than the steady-state ARL. Therefore, judging these charts by only using zero-state ARL values is misleading. From all synthetic profiles we conclude that the steady-state ARL is a much more representative measure than the more popular zero-state ARL, in particular for S_4 . Turning to the established competitor, we look at the EWMA profiles (two-dash and dotted line for $\lambda = 0.25$ and $= 0.1$, respectively). These two profiles reside clearly below all synthetic-type chart counterparts. Thereby, the $\lambda = 0.1$ EWMA is slightly better than the $\lambda = 0.25$ one (will change for larger δ). Eventually, the Shewhart chart ARL at $\delta = 1$ is with 54.58 too large to be seen in Figure 2.

We conclude that for $\delta = 1$, the “old” EWMA control chart exhibits the best performance. Later we will see that the version with $\lambda = 0.25$ does a good job for all considered shifts. For smaller shifts $\delta < 1$, the advantage of EWMA is even more pronounced. Before looking at larger changes, we want to emphasize that S_2 and S_3 show nearly the same profiles, with a slight advantage for the latter.

For the larger change $\delta = 2$ (see Figure 3), there are some clear overlappings between the synthetic and EWMA profiles. However, for changes at $\tau > 20$ (remind here the in-control ARL 500), the EWMA chart with $\lambda = 0.25$ is again the clear winner (for S_4 , $\tau > 3$ suffices). Note that the synthetic-type chart ($S_1, S_2,$

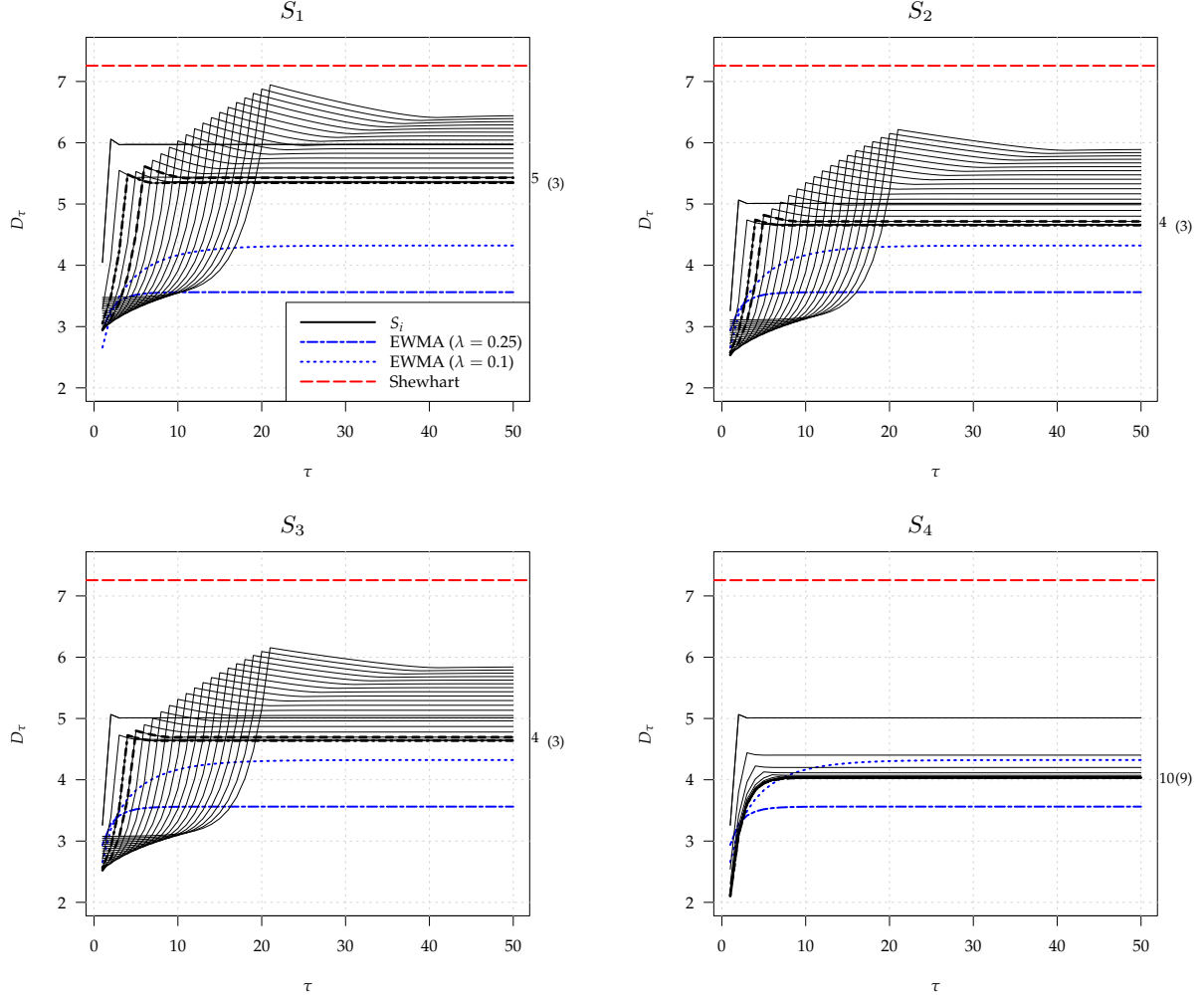


Figure 3: D_τ profiles for four synthetic-type charts with head-start, $H = 1, 2, \dots, 25$, best scheme (zero-state and steady-state) bold (dashed and dash-dotted) lines, shift $\delta = 2$, two EWMA charts; in-control ARL 500.

S_3) configurations which perform better than EWMA for $5 \leq \tau \leq 20$, exhibit heavily distorted performance for later changes, $\tau > 20$, which relegates them clearly from the competition. The EWMA chart with the smaller $\lambda = 0.1$ can compete with S_1 , S_2 and S_3 , but not with most of the S_4 designs. Thus, the actual competition is between the synthetic-type schemes and an EWMA chart with a mid-size λ . Before discussing the profiles of the former more in detail, we want to note that all charts behave better than the Shewhart chart (now its CED profile is visible). Except for S_4 , the differences between the profiles and within them are much more pronounced. The optimal H values are now smaller than for $\delta = 1$, that is we obtain for the zero-state ARL $H = 5, 4, 4, 10$ and for the steady-state ARL $H = 3, 3, 3, 9$ for S_1, \dots, S_4 , respectively. It is interesting that nearly the same H makes the considered ARL types minimal, for each chart type. In sum we conclude that for $\delta = 2$, EWMA ($\lambda = 0.25$) is practically the best performing chart with S_4 (and $H > 2$) on the second place. For all four synthetic-type charts, choosing $H \in \{4, 5, 6, 7\}$ seems to be a good choice.

Next, we look at the change $\delta = 3$, where the Shewhart chart yields the smallest ARL (which resembles zero-state, steady-state and all CED values). In Figure 4 we see similar patterns as before in Figure 3. Starting with S_1 , S_2 and S_3 , we observe the same (even much more) pronounced step shift of D_τ for S_1 , S_2 , S_3 at $\tau = H + 1$. The best configuration, in terms of both ARL types, is either $H = 2$ or 3 . The zero-state ARL (equal to D_1 , of course) and the CED value D_2 are lower than for EWMA ($\lambda = 0.25$), whereas for $\tau > 2$, the latter chart exhibits the smallest D_τ including its limit, the steady-state ARL. Thus, again EWMA dominates over these three synthetic-type charts clearly. The same has to be said about S_4 and EWMA ($\lambda = 0.25$), except for the supplemental D_3 , where both feature similar values. For all four synthetic-type

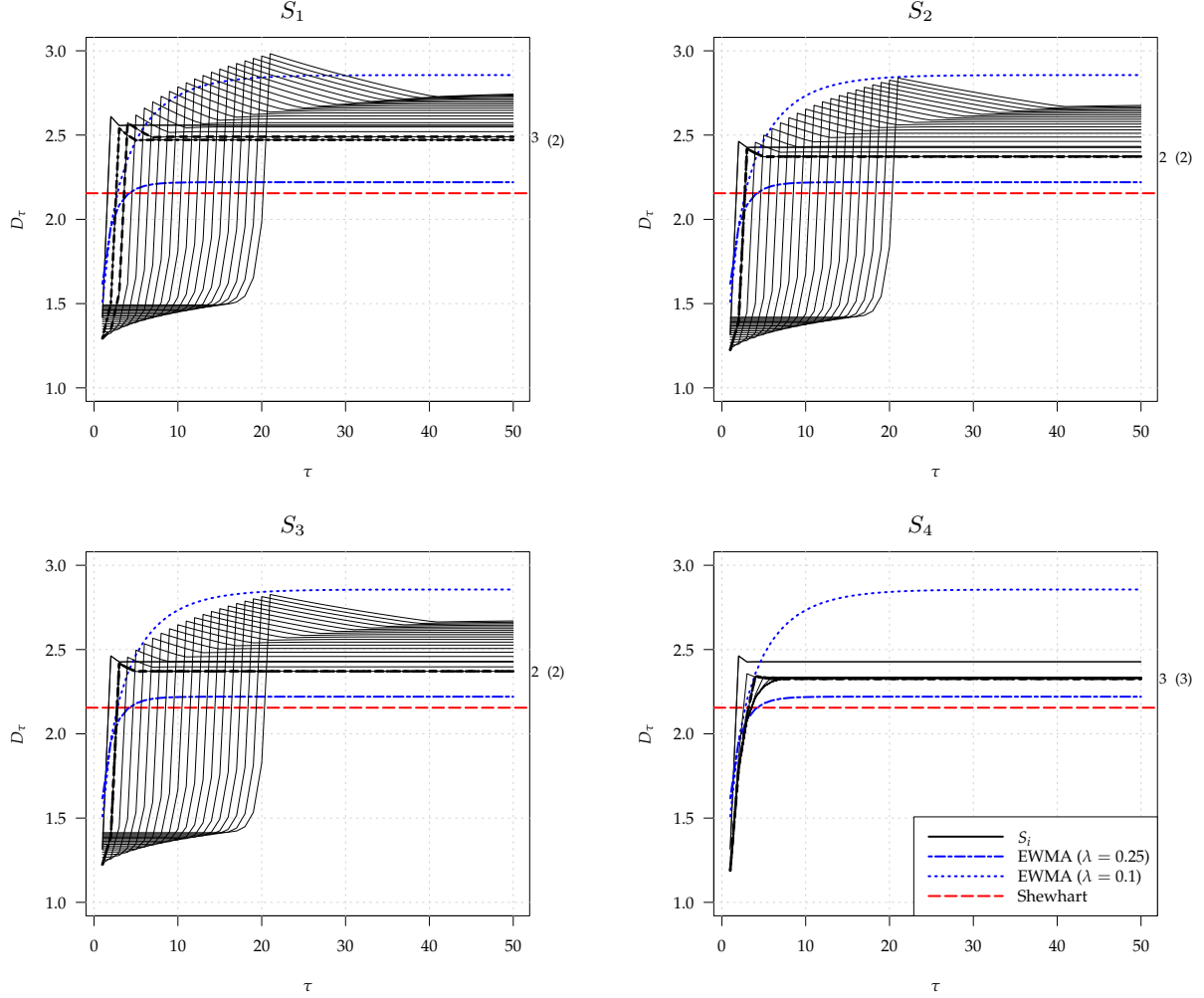


Figure 4: D_τ profiles for four synthetic-type charts with head-start, $H = 1, 2, \dots, 25$, best scheme (zero-state and steady-state) bold (dashed and dash-dotted) lines, shift $\delta = 3$, two EWMA charts; in-control ARL 500.

charts with head-start we encounter, in case of the optimal setups with $H \in \{2, 3\}$, really low values for $E_1(L) = D_1, D_2$ and (only for S_4) D_3 . But for every change after $\tau = 3$, the EWMA ($\lambda = 0.25$) chart beats all other charts under study. Thus, synthetic-type charts could be recommended only for the very special situation of early changes ($\tau \leq 3$) with considerable magnitude ($\delta \geq 2$). Else the classical EWMA chart with a mid-size $\lambda = 0.25$ is a better choice. Taking the ARL of the Shewhart chart into account, we conjecture that even a combination of synthetic-type charts and Shewhart charts (called improved synthetic charts in [Rakitzis et al., 2019](#)) will not be much better, for changes $\delta < 2$. Before we, however, provide our final judgment, some more comparisons (for a larger set of δ values) focusing on zero- and steady-state ARL will be performed. To make presentation more concise, we focus to type #4 charts, i.e. AR and MSS or R_4 and S_4 , respectively. Thus we include as well the no head-start version (AR) proposed by [Antzoulakos and Rakitzis \(2008\)](#).

To allow some overall judgment, we calculate ARL envelopes ([Dragalin, 1994](#)) for R_4 and S_4 . In detail, for each δ (on a rather fine grid) we pick H making the related out-of-control ARL minimal. The corresponding ARL values form the R_4 and S_4 envelope, respectively. In the here following Table 3, we present some examples for these H . We obtained the results by searching over $H \in \{1, 2, \dots, 200\}$. Because for small and mid-size δ , the ARL minimum is achieved for quite large H while simultaneously the changes from $H = 5$ on are nearly negligible, we replace the “global” H by the smallest member of the above set, where the corresponding ARL is not larger by 0.1% than the overall minimum. We deployed the same approach for the values given in Figures 2, 3 and 4 for S_4 . It is not surprising that R_4 and S_4 exhibit nearly the same optimal H values. Additionally, aiming at small zero- and steady-state ARLs results in similar H choices too. In the

Table 3: Optimal values of H for minimizing zero- and steady-state out-of-control ARL; in-control zero-state ARL is set to 500.

δ	0.25	0.5	0.75	1	1.5	2	2.5	3	4	5
zero-state										
R_4	12	15	17	17	14	8	4	3	2	2
S_4	12	15	18	19	15	10	6	3	2	2
steady-state										
R_4	12	15	17	17	14	9	5	3	2	4
S_4	12	15	17	18	14	9	5	3	2	4

appendix, we provide in Figure 9 two diagrams illustrating the dependence of the optimal H from δ in a more elaborated way. Here we want to emphasize that the actual choice of H is not really important, as long as it is not too small. Thus, some $5 \leq H \leq 10$ does the job sufficiently well. For the envelope, however, we use the best choice over $H \in \{1, 2, \dots, 200\}$.

Turning now to Figure 5 presenting the envelopes, we want to note that besides the already utilized EWMA chart with alarm rule (2) we deploy as well an EWMA chart with constant limits, namely with alarm condition $\tilde{c}_E \sqrt{\lambda/(2-\lambda)}$ relying on the asymptotic standard deviation of the EWMA statistics. Thereby, the factor $\tilde{c}_E = 2.998$ is slightly smaller than $c_E = 3.000$ in (2) for the same in-control zero-state ARL ($A = 500$). The fixed limits EWMA as the antagonist of R_4 is more popular in SPM literature and related software packages, because the ARL is more feasible (numerically). In Figure 5, we consider $0 < \delta \leq 5$. From the envelope

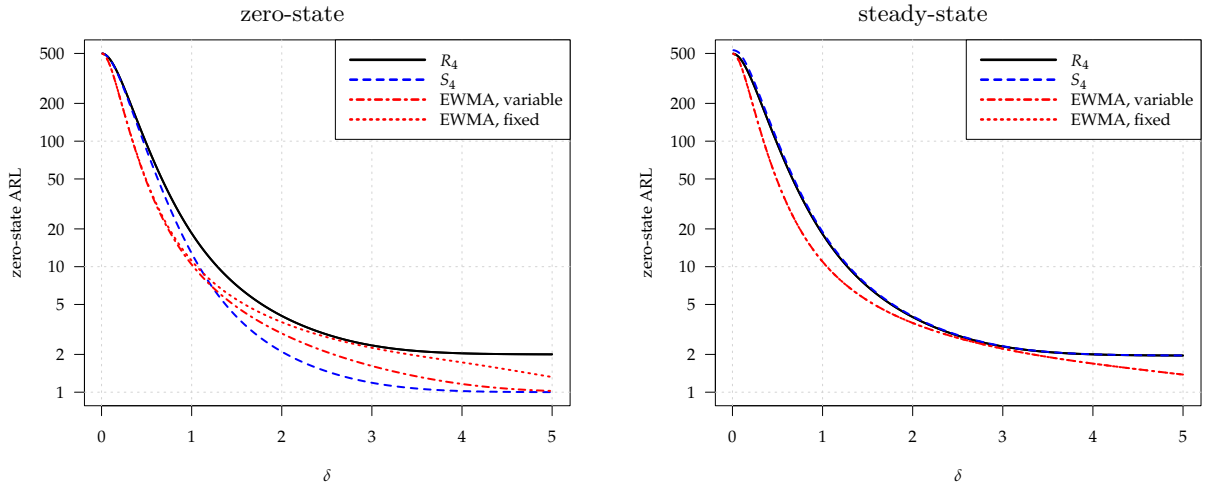


Figure 5: ARL Envelopes (point-wise minimal, $ARL \rightarrow \min_{1 \leq H \leq 200}$) of R_4 and S_4 (alias AR and MSS); in-control ARL 500; EWMA (E) with $\lambda = 0.25$.

diagram for the zero-state ARL we may conclude the popular statement that synthetic-type charts, here S_4 in particular, perform well for change sizes $\delta > 1$. These statements, however, are only valid for the head-start versions S_i . From Figures 2, 3 and 4 we know that this advantage vanishes as soon the change does not take place during the first few (less than 10) observations. That is, for most of the change point positions, the steady-state ARL is much more representative. Looking at the corresponding ARL envelope on the right-hand side of Figure 5 we conclude that EWMA with $\lambda = 0.25$ uniformly dominates the **point-wise** best R_4 and S_4 configurations. Besides, now the charts with head-start (S_4 , EWMA with (2) limits) and without head-start (R_4 , EWMA with fixed limits) behave alike. Interestingly, the steady-state ARL values for $2 \leq \delta \leq 3$ do not differ considerably between EWMA and the #4 charts. But for smaller **and** larger values of δ , EWMA performs much better than R_4/S_4 . While there is some remedy for the large values of δ , nothing helps to improve the synthetic-type charts for changes smaller than $\delta \leq 2$. The dominating competitor is a standard EWMA chart with $\lambda = 0.25$, which could be even tuned to improve either the performance for smaller or larger δ . Eventually we want to remember that changes of size $\delta \geq 3$ constitute the realm of Shewhart control

charts. In sum, synthetic-type charts (here #4) feature a decent detection performance for mid size changes, uniformly dominated by common EWMA control charts and partially overshadowed by Shewhart charts.

Next, we want to deal with the combination of synthetic-type charts and Shewhart charts, which was proposed in Rakitzis et al. (2019), and earlier in Wu et al. (2010) and Shongwe and Graham (2016). As we will later see, it improves the out-of-control steady-state ARL results for $\delta > 3$, helping to close the gap between the right tails in Figure 5. The adoption of the Markov chain models applied for all synthetic-type charts for incorporating the Shewhart limit is straightforward (Shongwe and Graham, 2016, 2017). It is more difficult for Shewhart-EWMA charts, but the Markov chain approximation described in Lucas and Saccucci (1990) works sufficiently well. We deploy here the more accurate algorithm introduced by Capizzi and Masarotto (2010). In order to illustrate the potential impact of adding the Shewhart rule, we consider for R_4 and S_4 the case $H = 6$, which is a reasonably general choice. Besides the above single EWMA charts with $\lambda = 0.25$ (exact and fixed limits), we consider a Shewhart-EWMA combo with $\lambda = 0.25$, Shewhart limit $k_2 = 3.25$ and EWMA threshold $\tilde{c}_E = 3.2097$ (in-control ARL 500), where the EWMA component features constant limits (otherwise ARL calculation becomes more complicated). For the two synthetic-type charts we look at many combinations of (k_1, k_2) , where k_1 replaces k in (4) and k_2 is again the Shewhart limit (of course, $k_2 > k_1$). We start with $k_2 = 3.1$ (the limit for a standalone Shewhart chart with in-control ARL 500 is $k_2 = 3.09$) and increase it by 0.02 steps (up to 7). The k_1 of the inner synthetic rule is determined (for $H = 6$) to attain the in-control zero-state ARL 500 of the combo. The resulting bundles of Shewhart-#4 charts provide the grey areas in Figure 6, where two members are highlighted. The black solid line marks

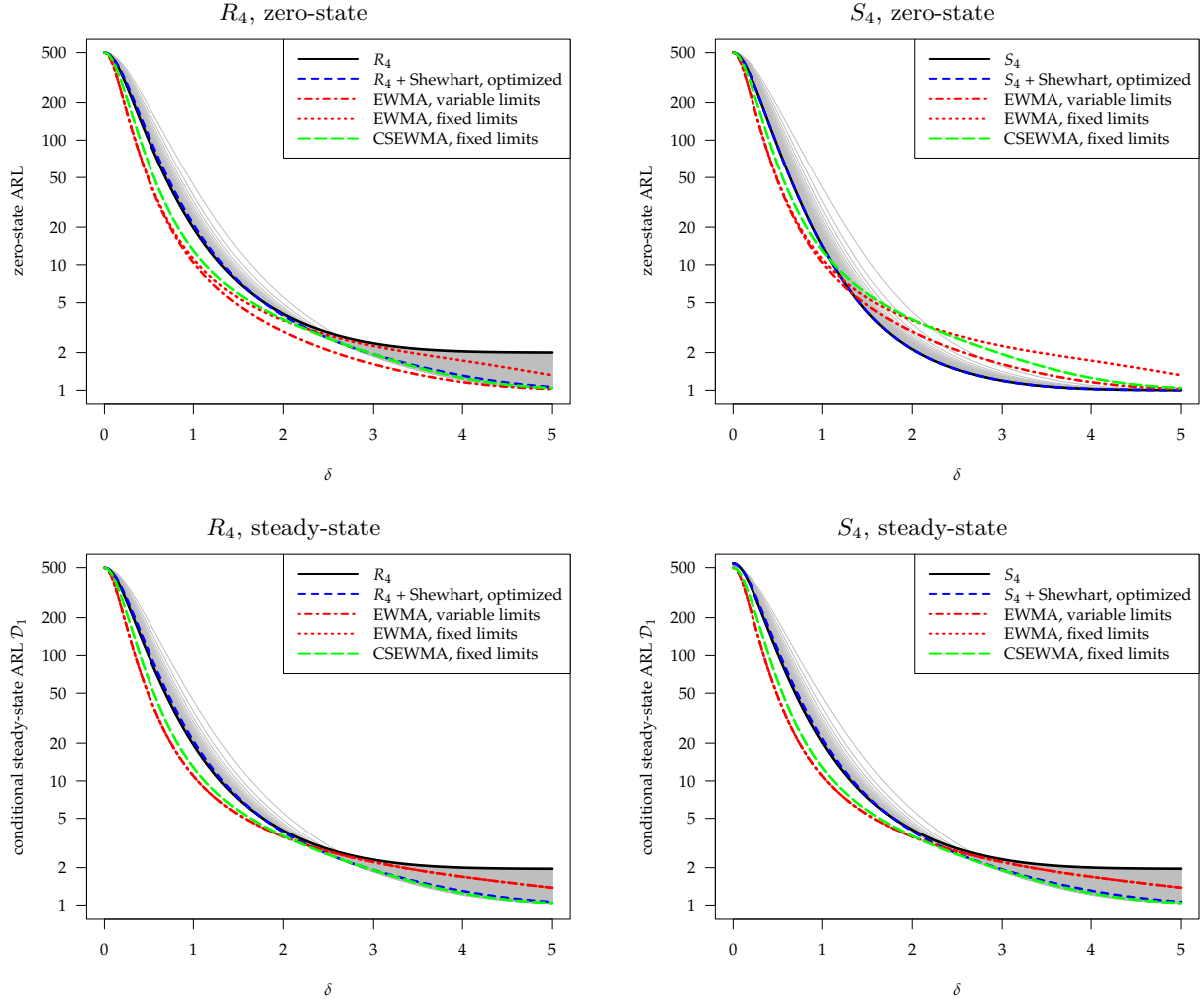


Figure 6: ARL performance of single charts and combos; #4 charts with $H = 6$, EWMA with $\lambda = 0.25$; in-control ARL 500.

the original pure #4 chart, whereas the blue dashed lines presents an optimal member. Optimal means here, that the measure $EQL = 1/\delta_{\max} \sum_i \delta_i^2 ARL_i$ is minimized (ARL_i is the out-of-control ARL for shift δ_i). The utility function EQL was used in [Shongwe and Graham \(2016\)](#) in order to evaluate the detection performance over a range of shifts with a single number. We set $\delta_{\max} = 5$ and $\delta_i = 0.01i$. The impact of small shifts (our $\delta_1 = 0.01$ is really small) to EQL is rather minuscule because of the weights δ_i^2 . The resulting Shewhart limits k_2 are 4.78 for S_4 in case of the zero-state ARL, 3.46 in case of the steady-state ARL, and 3.48 for R_4 in both cases. Only the first value, $k_2 = 4.78$ sticks out, which does not really surprise because the zero-state performance of the head-start scheme S_4 is already sound. The other numbers are quite similar. And for R_4 it is not important, what ARL measure is utilized. We recognize the improvement potential for shifts $\delta \geq 3$ (the Shewhart realm). The best Shewhart-#4 charts exhibit profiles that are slightly lifted for changes $\delta \leq 2$ and substantially lowered for $\delta \geq 3$. For the Shewhart- R_4 combo we observe quite similar patterns for the zero-state and the steady-state ARL. It is different for Shewhart- S_4 , where many members of the aforementioned Shewhart- S_4 family yield agreeably small ARL values for $\delta > 1$. We notice as well that the standalone EWMA chart with exact limits, see (2), exhibits the best uniform performance within the EWMA charts. But the other two entertain constant limits, which results in higher zero-state ARL values by construction. However, the more interesting comparison is the one for the steady-state ARL. And here we conclude that all three EWMA designs behave better for changes $\delta < 2$, again. For changes $2 \leq \delta \leq 3$, all considered charts perform similarly. And for large changes, $\delta > 3$, the combo schemes (Shewhart-#4 and Shewhart-EWMA) are the best ones and display roughly the same performance. Then the two standalone EWMA charts follow, as we observed already in Figure 5. The worst chart types are the standalone #4 charts (R_4/S_4). In summary, the merge of Shewhart with synthetic-type charts helps to close the $\delta > 3$ ARL gap. However, the Shewhart-EWMA combo shows much better performance for changes $\delta \leq 2$, whereas for larger changes it behaves like the optimal Shewhart-#4. Thus, a clear recommendation could be given: Use either single EWMA or Shewhart-EWMA combo charts.

Finally, we want to stress the expedience of choosing the so-called wildcard head-start in contrast to the standard setup, which was chosen without further ado for the R_i charts, namely DR, KL, MC1 and AR by [Derman and Ross \(1997\)](#), [Klein \(2000\)](#), [Machado and Costa \(2014\)](#) and [Antzoulakos and Rakitzis \(2008\)](#), respectively. While the majority of the runs rules chart literature picked this initial state, which resembles the worst-case (maximum out-of-control ARL), [Wu and Spedding \(2000b\)](#) started a movement to chose the best-case state. In the here following Figure 7 we illustrate, how quickly the control charts “return” to the worst-case after starting in the best-case. For an in-control ARL of 500 we plot the probability that after i observations the synthetic chart arrives in the worst-case state. With \mathfrak{S}_i we denote the state at observation i . From Table 2 we know the number of possible states (for the simple #1 chart, we observe 0 and H as best- and worst-case state following the notation in (4), that is, picking the states from the set $\{0, 1, \dots, H\}$). To improve presentation, we started plotting at this i , where the said probability is positive. Interestingly, for S_1 , S_2 and S_3 , we obtain $P(\mathfrak{S}_i = \text{worst-case} \mid L > i) = 0$ for $i < H$ and $P(\mathfrak{S}_H = \text{worst-case} \mid L > H) = 1$. If there is no (false) alarm during the first H observations, then we reach the worst case state with probability 1 at the H th observation. Thus, the behavior of the head-start and the common design differs substantially only during the first H observations. Then the head-start type chart arrives in the worst-case state with (conditional) probability one. The common chart started in the worst-case with probability one, but returns to it at index H with a (conditional) probability, which is quite large, but smaller than one. The bullets at the end of all profiles in Figure 7 mark the conditional steady-state probability of the worst-case. For all four chart types and all considered $H = 1, 2, \dots, 20$ the convergence to the latter values is quick. Eventually, we put a bullet too at $P(\mathfrak{S}_H = \text{worst-case} \mid L > H)$ for all four chart types.

The S_4 chart differs slightly from the other ones. First, only for $H = 1$ we observe $P(\mathfrak{S}_H = \text{worst-case} \mid L > H) = 1$. For larger H , we neither get long series of zero probabilities (from $i = 2$ on the probability is positive) nor the probability one at $i = H$. But more importantly, the dominating probability value is about 92%. Thus the best design among all considered synthetic-type charts with head-start, namely S_4 , exhibits two faces: (i) It shows an excellent zero-state ARL profile, cf. to Figure 5. (ii) But these low values are highly untypical facets of S_4 , because it operates with a probability of more than 90% in worst-case mode. Thus, a thorough and legitimate judgment of the S_4 chart would rely on the ARL numbers we know for the no head-start version, i.e. for R_4 . Another way of avoiding misjudgment is, of course, considering the steady-state ARL. Finally we should mention that for S_1 , S_2 and S_3 a similar statement could be given, because the deplorable probability of being in the worst-case is not much smaller, it is for all considered configurations larger than 75%.

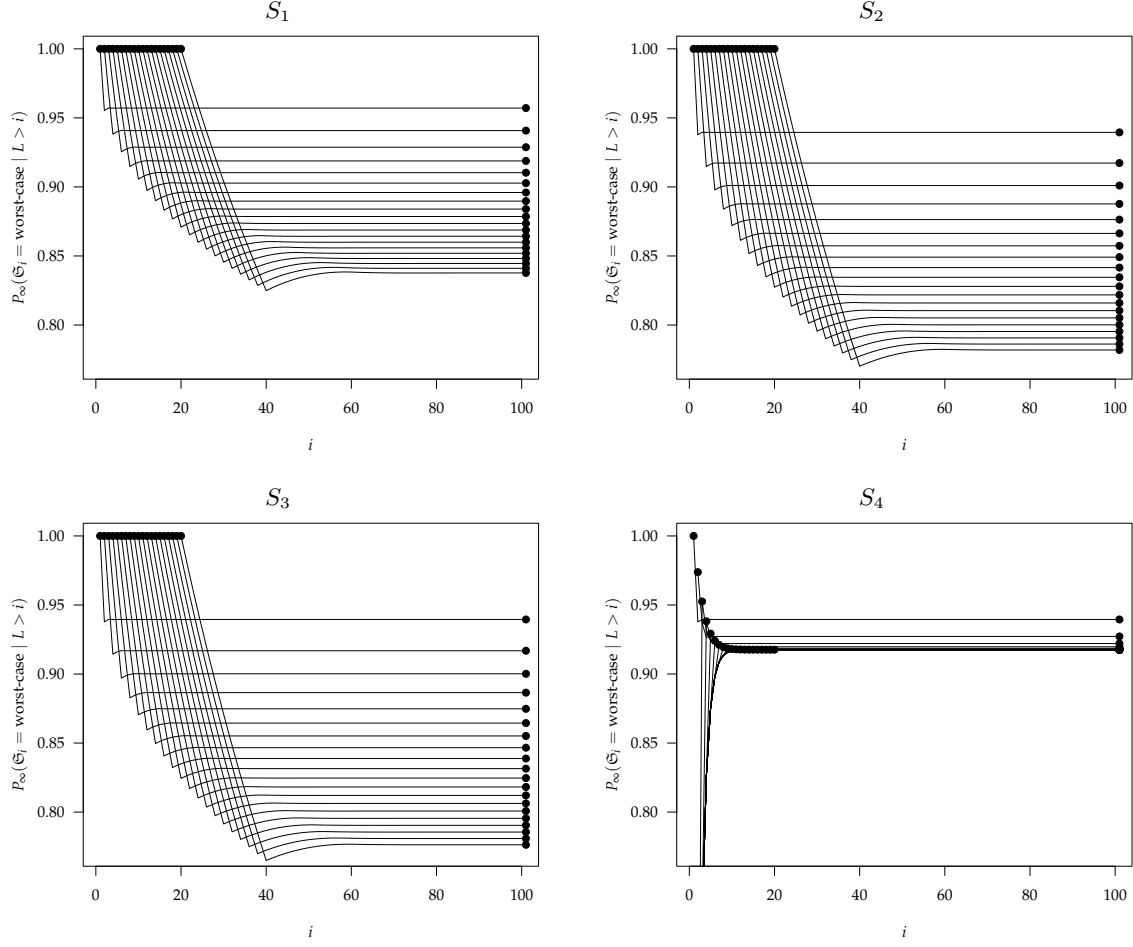


Figure 7: Conditional (in-control) probability of being in the worst-case state, $P_\infty(\mathfrak{S}_i = \text{worst-case} \mid L > i)$; in-control ARL 500, $H = 1, 2, \dots, 20$, the larger H the lower the asymptotic level.

5 Conclusions

Of course, synthetic-type charts (R_1, \dots, S_4) are easy to build and to analyze. In particular, for the analysis one can easily apply exact Markov chain models. For the simplest ones, R_1 and S_1 , there are even explicit solutions for all considered measures. EWMA control charts, however, are similarly easy to use. Their ARL analysis needs more computational power, which is not a problem nowadays. Detection performance-wise, a clear recommendation can be given: Apply EWMA, because it exhibits the best detection performance for small changes $\delta \leq 1.5$ (in terms of standard deviation) in our study, whereas for larger changes all the considered schemes differ not much. Without an added Shewhart rule, synthetic-type charts perform worse than EWMA even for large changes ($\delta > 3$). Adding this Shewhart rule improves the large change detection behavior a lot, for both synthetic-type (here we focus to R_4 and S_4 , the most recent phenotypes) and EWMA control charts. Finally we want to urgently emphasize that for a sound analysis of a control chart device dealing with the steady-state ARL is adamant. Naturally, a worst-case ARL analysis would be appropriate too. The R_i charts are designed through the lens of their worst-case ARL. In Appendix A.3 a rough comparison between R_4 and CUSUM (cumulative sum charts introduced in Page, 1954) control charts (the worst-case “experts”) is provided. Again, the older charts (CUSUM) yield better ARL results. In summary, synthetic-type charts are somewhat easier to setup than the classical charts such as EWMA and CUSUM, but the older ones exhibit the better detection performance.

References

- Antzoulakos, D. L. and Rakitzis, A. C. (2008). The modified r out of m control chart. Communications in Statistics – Simulation and Computation, 37(2):396–408.
- Bersimis, S., Koutras, M. V., and Rakitzis, A. C. (2020). Run and scan rules in statistical process monitoring. In Glaz, J. and Koutras, M. V., editors, Handbook of Scan Statistics, pages 1–32.
- Brook, D. and Evans, D. A. (1972). An approach to the probability distribution of CUSUM run length. Biometrika, 59(3):539–549.
- Capizzi, G. and Masarotto, G. (2010). Evaluation of the run-length distribution for a combined Shewhart-EWMA control chart. Statistics and Computing, 20(1):23–33.
- Chakraborti, S. and Rakitzis, A. C. (2021). Control charts, synthetic. In Wiley StatsRef: Statistics Reference Online, pages 1–18.
- Crosier, R. B. (1986). A new two-sided cumulative quality control scheme. Technometrics, 28(3):187–194.
- Crowder, S. V. (1987). A simple method for studying run-length distributions of exponentially weighted moving average charts. Technometrics, 29(4):401–407.
- Darroch, J. N. and Seneta, E. (1965). On quasi-stationary distributions in absorbing discrete-time finite Markov chains. Journal of Applied Probability, 2(1):88–100.
- Davis, R. B. and Woodall, W. H. (2002). Evaluating and improving the synthetic control chart. Journal of Quality Technology, 34(2):200–208.
- Derman, C. and Ross, S. M. (1997). Statistical Aspects of Quality Control. Academic Press.
- Dragalin, V. (1994). Optimal CUSUM envelope for monitoring the mean of normal distribution. Econ. Qual. Control, 9(4):185–202.
- Klein, M. (2000). Two alternatives to the Shewhart \bar{X} control chart. Journal of Quality Technology, 32(4):427–431.
- Knoth, S. (2003). EWMA schemes with non-homogeneous transition kernels. Sequential Analysis, 22(3):241–255.
- Knoth, S. (2005). Fast initial response features for EWMA control charts. Statistical Papers, 46(1):47–64.
- Knoth, S. (2016). The case against the use of synthetic control charts. Journal of Quality Technology, 48(2):178–195.
- Knoth, S. (2018). New results for two-sided CUSUM-Shewhart control charts. In Frontiers in Statistical Quality Control 12, pages 45–63. Springer International Publishing.
- Knoth, S. (2021a). spc: Statistical Process Control – Collection of Some Useful Functions. R Foundation for Statistical Computing, Vienna, Austria. R package version 0.6.5.
- Knoth, S. (2021b). Steady-state average run length(s) — methodology, formulas and numerics. Sequential Analysis, 40(3):405–426.
- Lucas, J. M. and Saccucci, M. S. (1990). Exponentially weighted moving average control schemes: Properties and enhancements. Technometrics, 32(1):1–12.
- Machado, M. A. G. and Costa, A. F. B. (2014). Some comments regarding the synthetic \bar{X} chart. Communications in Statistics – Theory and Methods, 43(14):2897–2906.
- Montgomery, D. C. (2019). Introduction to Statistical Quality Control. Wiley, Hoboken, NJ.
- Page, E. S. (1954). Continuous inspection schemes. Biometrika, 41(1-2):100–115.
- Rakitzis, A. C., Chakraborti, S., Shongwe, S. C., Graham, M. A., and Khoo, M. B. C. (2019). An overview of synthetic-type control charts: Techniques and methodology. Quality and Reliability Engineering International, 35(7):2081–2096.
- Roberts, S. W. (1959). Control chart tests based on geometric moving averages. Technometrics, 1(3):239–250.
- Shewhart, W. A. (1925). The application of statistics as an aid in maintaining quality of a manufactured product. J. Amer. Statist. Assoc., 20(152):546–548.
- Shongwe, S. C. and Graham, M. A. (2016). On the performance of Shewhart-type synthetic and runs-rules charts combined with an \bar{X} chart. Quality and Reliability Engineering International, 32(4):1357–1379.

- Shongwe, S. C. and Graham, M. A. (2017). Synthetic and runs-rules charts combined with an \bar{X} chart: Theoretical discussion. *Quality and Reliability Engineering International*, 33(1):7–35.
- Shongwe, S. C. and Graham, M. A. (2018). A modified side-sensitive synthetic chart to monitor the process mean. *Quality Technology & Quantitative Management*, 15(3):328–353.
- Shongwe, S. C. and Graham, M. A. (2019). Some theoretical comments regarding the run-length properties of the synthetic and runs-rules \bar{X} monitoring schemes – part 2: Steady-state. *Quality Technology & Quantitative Management*, 16(2):190–199.
- Taylor, H. M. (1968). The economic design of cumulative sum control charts. *Technometrics*, 10(3):479–488.
- Wu, Z., Ou, Y., Castagliola, P., and Khoo, M. B. (2010). A combined synthetic \bar{X} chart for monitoring the process mean. *International Journal of Production Research*, 48(24):7423–7436.
- Wu, Z. and Spedding, T. A. (2000a). Implementing synthetic control charts. *Journal of Quality Technology*, 32(1):74–78.
- Wu, Z. and Spedding, T. A. (2000b). A synthetic control chart for detecting small shifts in the process mean. *Journal of Quality Technology*, 32(1):32–38.

A Appendix

A.1 Explicit formulae for steady-state ARL for S_1 (R_1) and its limit for $\delta \rightarrow 0$

Because in Shongwe and Graham (2016) the steady-state ARL was deployed to determine k , we look at the most simple case, namely S_1 (and implicitly R_1) more thoroughly, augmenting somehow Shongwe and Graham (2017, 2019). We consider all ψ_i , $i = 1, 2, 3, 4$ (see Section 3). The actual shift δ is added as subscript, for example $\psi_{1;0}$ denotes the in-control case $\delta = 0$.

Conditional steady-state ARL, cf. to Knoth (2016):

$$\mathcal{D}_1 = \psi'_{1;0} \ell_\delta = \left(\frac{q_0}{p_0} + \frac{1 - \left(\frac{q_0}{q_0} \right)^H}{1 - \frac{q_0}{q_0}} \right) \frac{s_0}{p_\delta} + \left(\frac{q_0}{p_0} + q_\delta^H \frac{1 - \left(\frac{q_0}{q_\delta q_0} \right)^H}{1 - \frac{q_0}{q_\delta q_0}} \right) \frac{s_0}{r_\delta} \xrightarrow{\delta \rightarrow 0} \frac{1}{1 - q_0}.$$

Cyclical steady-state ARL, re-start at state 0, cf. to Wu et al. (2010); Knoth (2016):

$$\mathcal{D}_2 = \psi'_{2;0} \ell_\delta = \frac{1 + q_0 p_\delta \frac{q_0^H - q_\delta^H}{q_0 - q_\delta}}{r_\delta} \xrightarrow{\delta \rightarrow 0} \frac{1 + H p_0 q_0^H}{r_0} = \frac{1}{r_0} + H \frac{q_0^H}{1 - q_0^H}.$$

Cyclical steady-state ARL, re-start at state H , cf. to Shongwe and Graham (2019):

$$\mathcal{D}_3 = \psi'_{3;0} \ell_\delta = \frac{1 - q_\delta^H}{r_\delta} + \frac{1 + p_0 q_\delta \frac{q_0^H - q_\delta^H}{q_0 - q_\delta}}{r_\delta (2 - q_0^H)} \xrightarrow{\delta \rightarrow 0} \frac{1 - q_0^H}{r_0} + \frac{1 + H p_0 q_0^H}{r_0 (2 - q_0^H)}.$$

Wrong conditional steady-state ARL, cf. to Shongwe and Graham (2017, 2019):

$$\mathcal{D}_4 = \psi'_{4;0} \ell_\delta = \frac{1 - q_\delta^H}{r_\delta} + \frac{1 + p_0 q_\delta \frac{1 - q_\delta^H}{1 - q_\delta}}{r_\delta (1 + H p_0)} \xrightarrow{\delta \rightarrow 0} \frac{1 - q_0^H}{r_0} + \frac{1 + q_0 (1 - q_0^H)}{r_0 (1 + H p_0)}.$$

Next we apply the above formulas for a S_1 chart with $H = 3$ and $k = 2.2238$ (in-control ARL 500). Besides the four different steady-state ARL results we show as well the zero-state ARL of an R_1 (alias true synthetic chart without head-start) in the following Table 4. The four \mathcal{D}_i values are nearly the same. Thus, using one

Table 4: In-control ARL for S_1 and R_1 , zero-state ℓ and steady-state \mathcal{D} , $H = 3$, $k = 2.2238$.

ℓ_{S_1}	ℓ_{R_1}	\mathcal{D}_1	\mathcal{D}_2	\mathcal{D}_3	\mathcal{D}_4
500	538.224	536.378	536.242	536.383	536.354

of the correct or even the wrong (\mathcal{D}_4) formulas makes not a big difference. Interestingly, the zero-state ARL

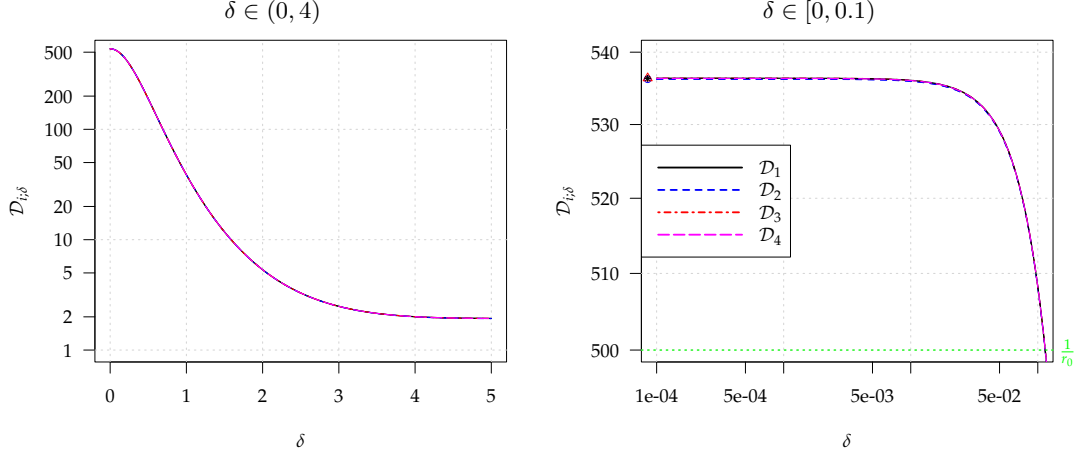


Figure 8: Various types of steady-state ARL, \mathcal{D}_i , for a typical range of changes $(0, 5)$ and for $\delta \rightarrow 0$, true synthetic chart (S_1) with $H = 3$ and $k = 2.2238$ (in-control ARL 500).

ℓ_{R_1} chart is really close to these numbers as well. Thus, for charts without head-start it is sufficient to look at the zero-state ARL (the mentioned behavior carries over to the out-of-control case).

To judge this behavior for the out-of-control case, we plotted in Figure 8 some \mathcal{D}_i profiles. Not surprisingly, all these profiles coincide. From these numbers we conclude that the wrongly chosen steady-state vector recipe in Shongwe and Graham (2017, 2019) does not induce visible consequences.

Eventually we want to mention that calibrating (setting k for synthetic-type charts) control charts to achieve a certain in-control steady-state ARL, as it was done in Shongwe and Graham (2016), refers to starting the chart from its steady-state distribution. This is certainly not a common task in SPM practice.

A.2 Minimizing out-of-control ARL by tuning H

In addition to the numbers given in Table 3 (Section 4) we show here the complete output of our optimization procedure. For both #4 charts (R_4 and S_4) we tried $H \in \{1, 2, \dots, 200\}$ and picked the H value that either minimizes the zero- or the steady-state ARL. In addition, we searched for small H values that yield ARL values not larger by 0.1% than the overall minimum. In Figure 9 all these H values are plotted. The in-control

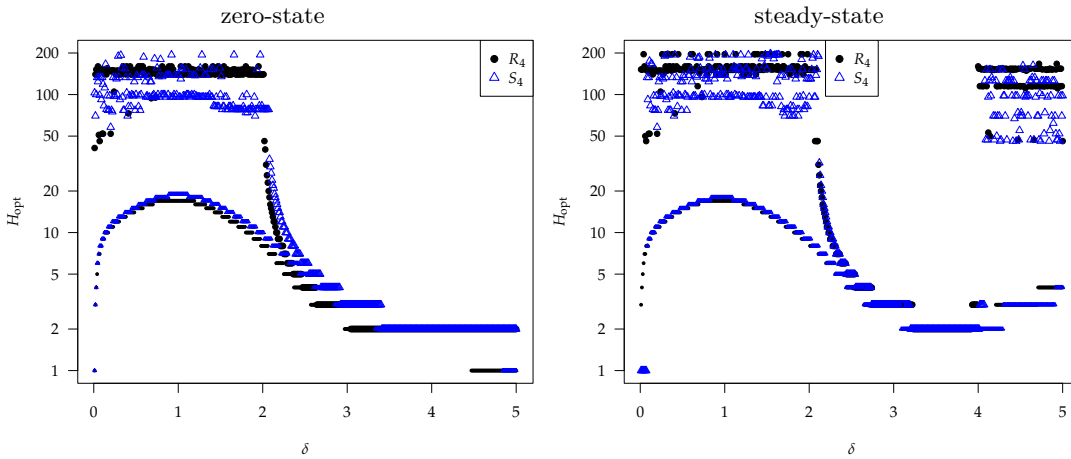


Figure 9: Optimal H values.

ARL is set to 500. We observe quite similar patterns for both ARL types. The most pronounced difference could be seen for $\delta > 4$. Fortunately, tuning synthetic-type charts for so large changes is quite uncommon.

A.3 Worst-case ARL competition

Here, we compare the zero-state ARL of R_4 ($H = 8$ – optimal for $\delta = 2$) and of two-sided CUSUM control charts. For the latter we choose $k = 1$ (k denotes here the reference value of a CUSUM control chart) to achieve good performance for mid-size changes ($\delta = 2$ and its neighborhood). We add as well a combo of R_4

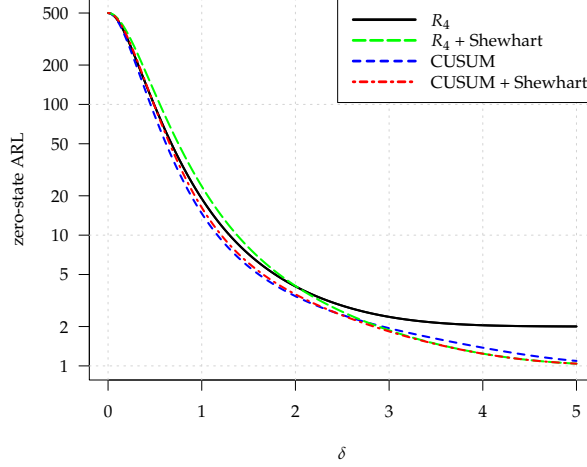


Figure 10: Zero-state ARL comparison between R_4 ($H = 8$) and CUSUM control charts ($k = 1$); in-control ARL 500; for both a combo version (+ Shewhart with alarm threshold $k_2 = 3.25$) is added.

and Shewhart ($k_2 = 3.25$) to deal with the weak right-hand tail of R_4 . The $k = 1$ CUSUM ($h = 2.665$) is uniformly better than R_4 . Compared to R_4 , the Shewhart- R_4 combo exhibits a better detection performance for $\delta \geq 3$. Finally, the Shewhart-CUSUM combo ($k = 1$, $k_2 = 3.25$ and $h = 2.947$) shows lower out-of-control ARL results for $\delta < 3$ and more or less the same values for $\delta \geq 3$ like the Shewhart- R_4 combo. Thus, the CUSUM schemes win both worst-case ARL competitions. Eventually we want to note that the ARL values of the Shewhart-CUSUM combo are determined with the algorithms given in [Knoth \(2018\)](#). For the standard CUSUM the function `xcusum.arl()` from the R package `spc` is utilized.

A.4 Further CED profiles

In addition to the cases $\delta \in \{1, 2, 3\}$ we plot here some CED profiles for further changes, namely $\delta \in \{0.5, 1.5\}$.

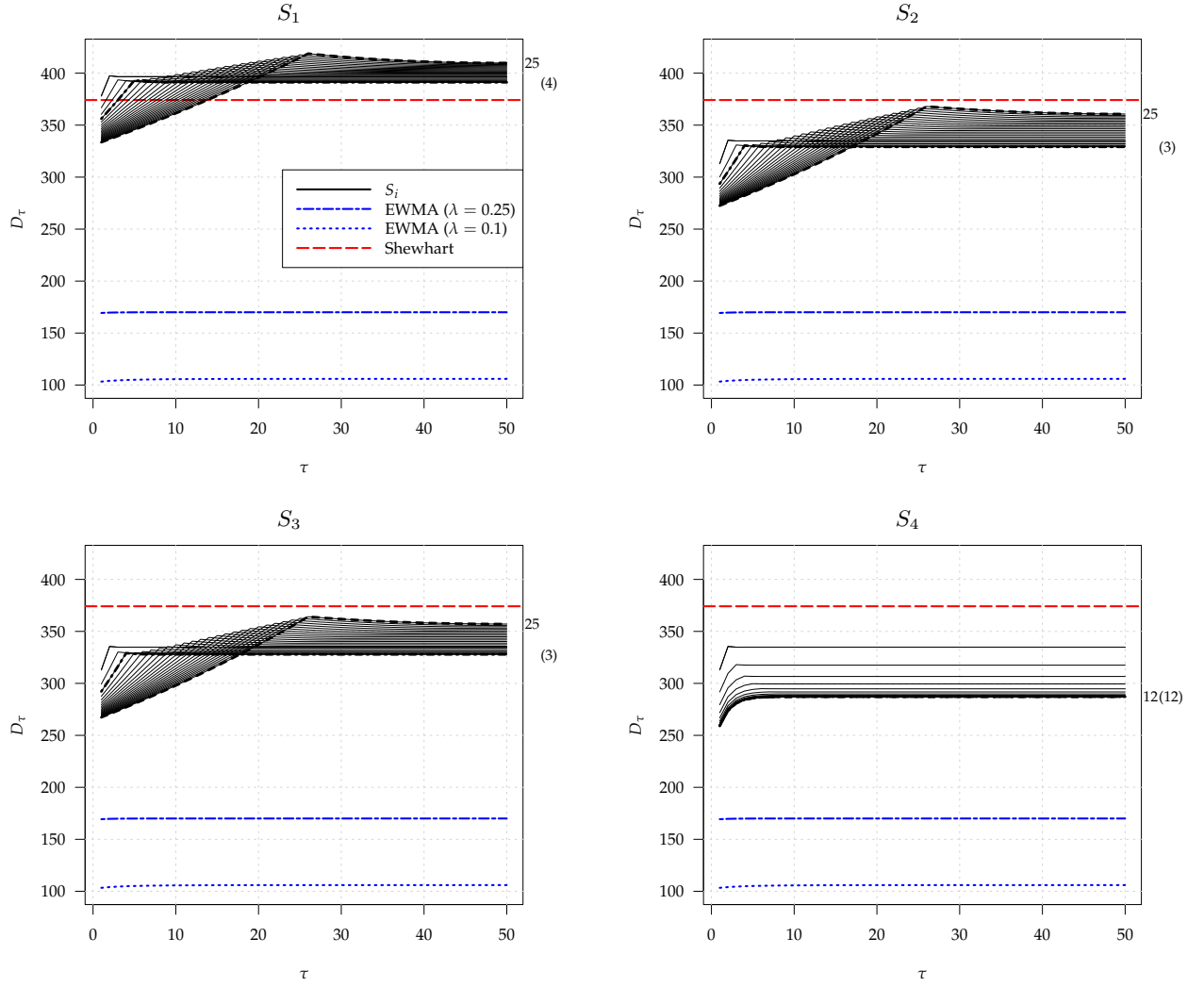


Figure 11: D_τ profiles for four synthetic-type charts with head-start, $H = 1, 2, \dots, 25$, best scheme (zero-state and steady-state) bold (dashed and dash-dotted) lines, shift $\delta = 0.25$, two EWMA charts; in-control ARL 500.

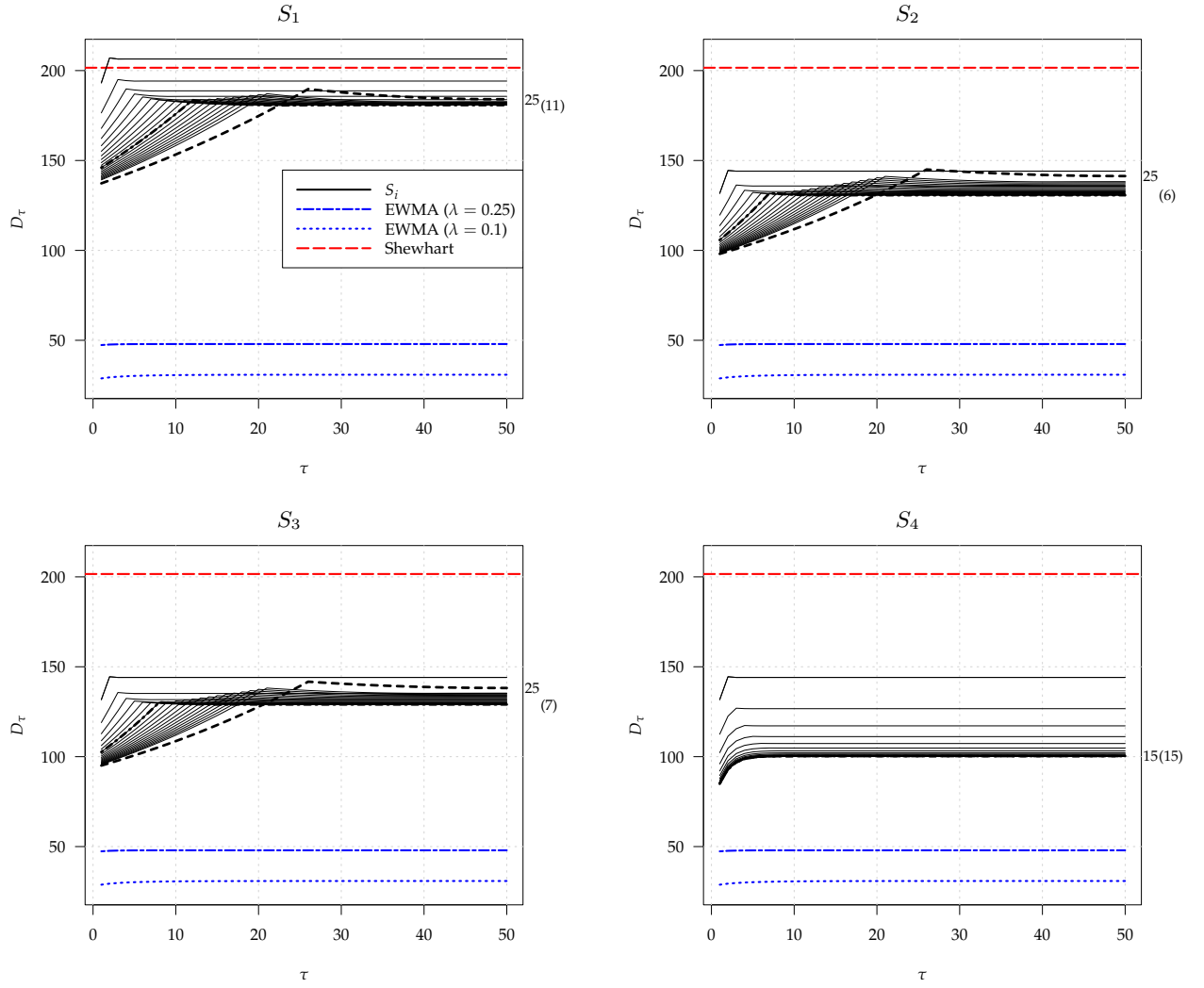
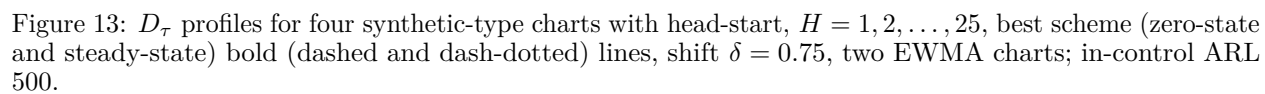


Figure 12: D_τ profiles for four synthetic-type charts with head-start, $H = 1, 2, \dots, 25$, best scheme (zero-state and steady-state) bold (dashed and dash-dotted) lines, shift $\delta = 0.5$, two EWMA charts; in-control ARL 500.



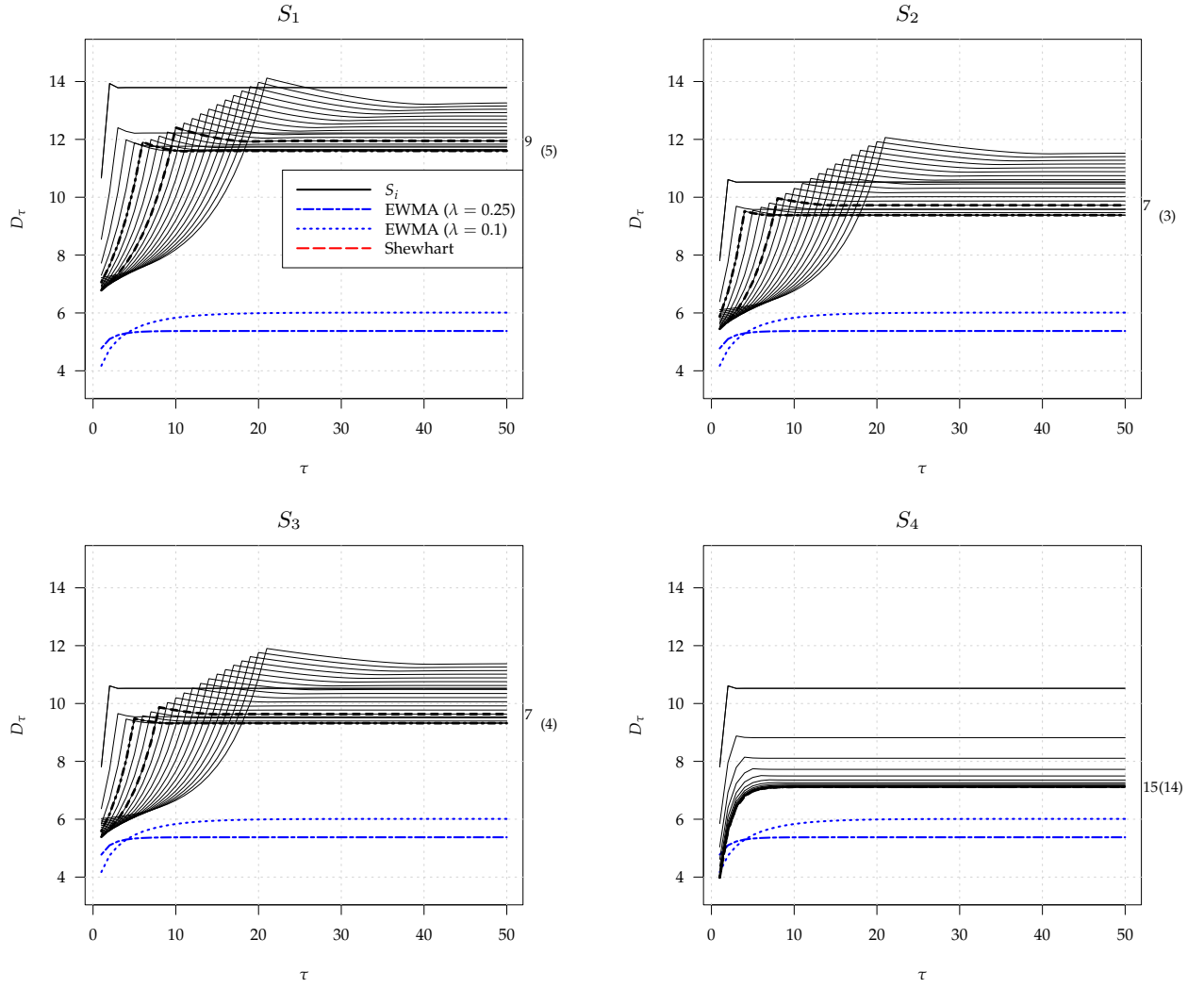


Figure 14: D_τ profiles for four synthetic-type charts with head-start, $H = 1, 2, \dots, 25$, best scheme (zero-state and steady-state) bold (dashed and dash-dotted) lines, shift $\delta = 1.5$, two EWMA charts; in-control ARL 500.

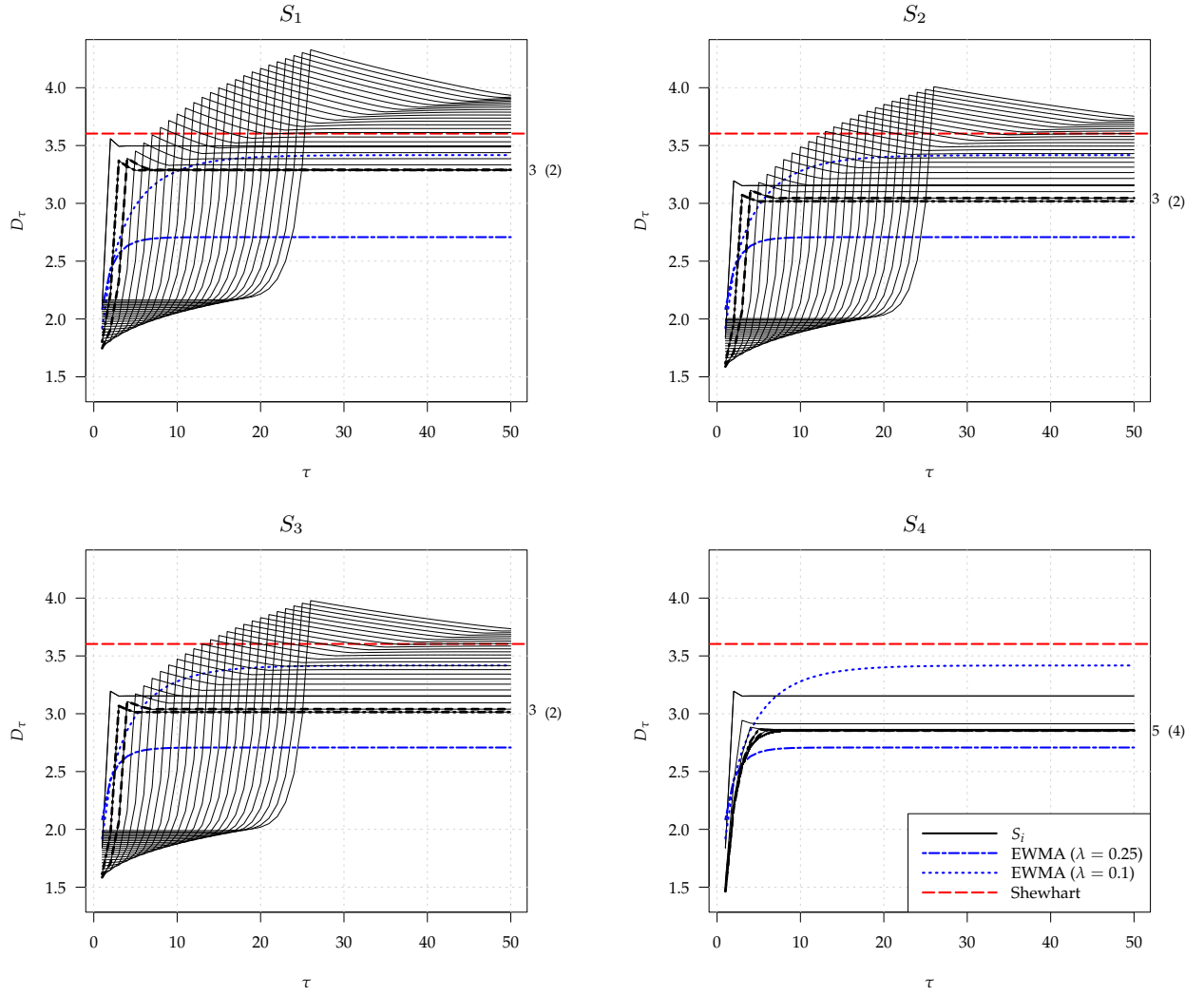


Figure 15: D_τ profiles for four synthetic-type charts with head-start, $H = 1, 2, \dots, 25$, best scheme (zero-state and steady-state) bold (dashed and dash-dotted) lines, shift $\delta = 2.5$, two EWMA charts; in-control ARL 500.

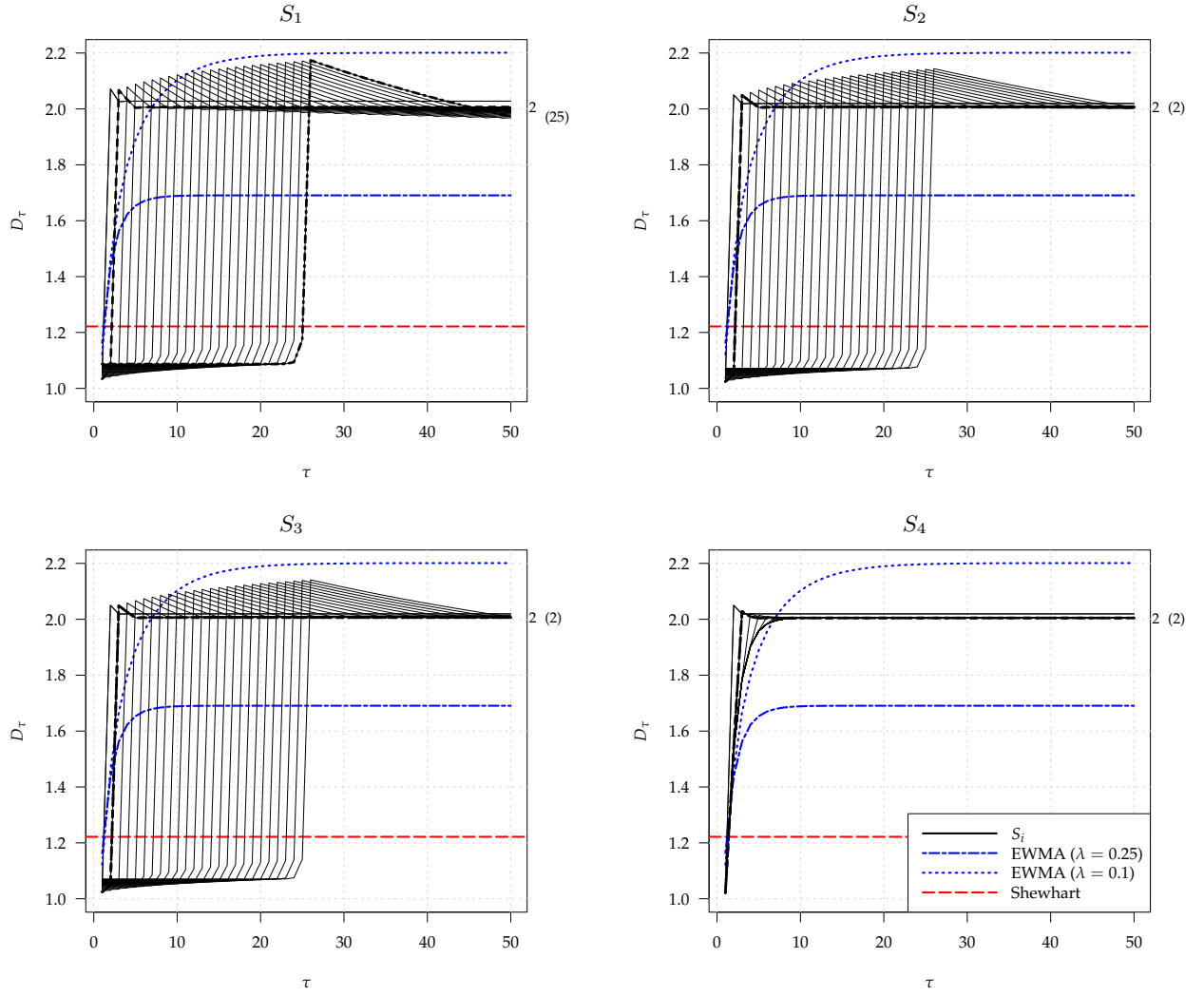


Figure 16: D_τ profiles for four synthetic-type charts with head-start, $H = 1, 2, \dots, 25$, best scheme (zero-state and steady-state) bold (dashed and dash-dotted) lines, shift $\delta = 4$, two EWMA charts; in-control ARL 500.

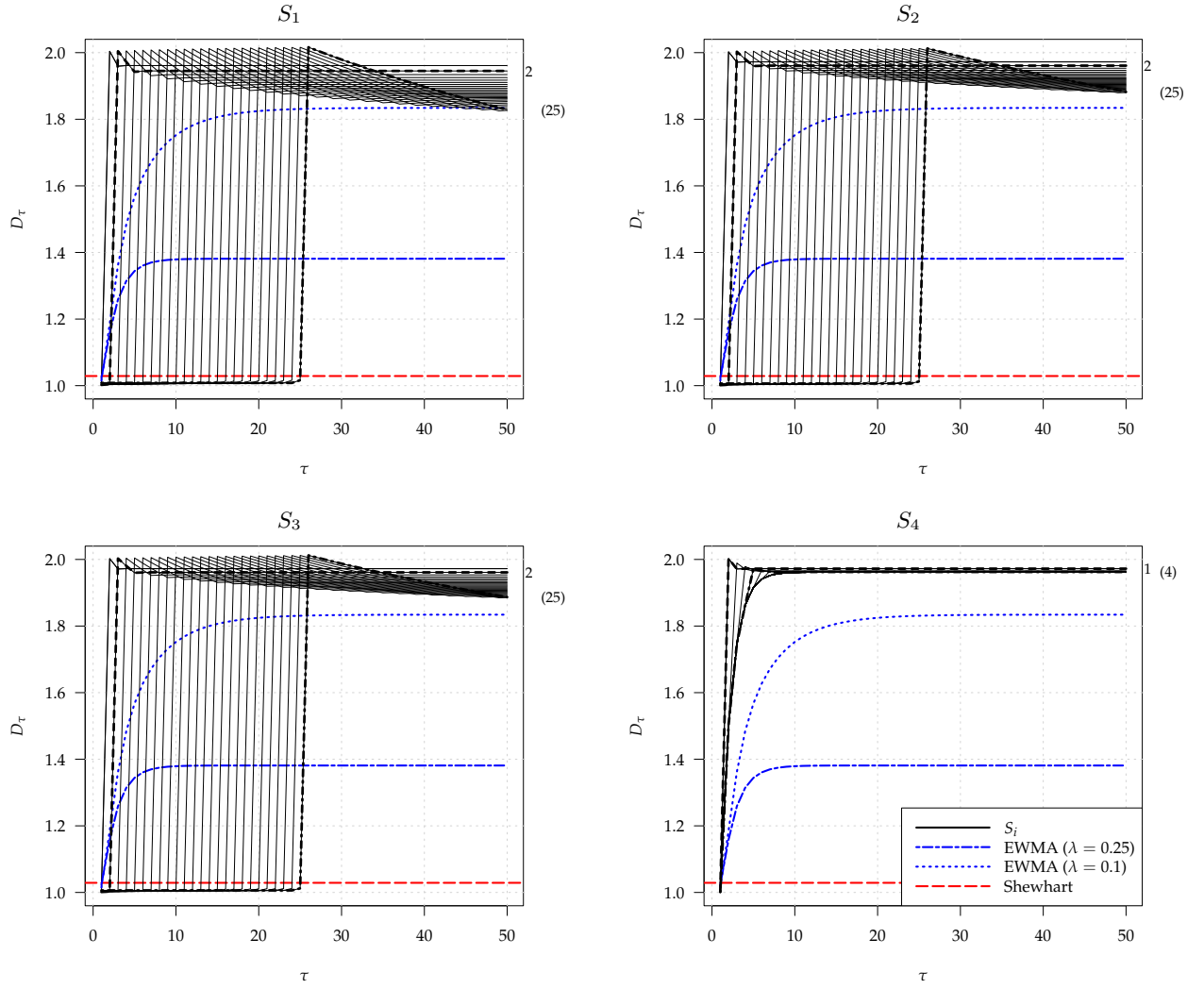


Figure 17: D_τ profiles for four synthetic-type charts with head-start, $H = 1, 2, \dots, 25$, best scheme (zero-state and steady-state) bold (dashed and dash-dotted) lines, shift $\delta = 5$, two EWMA charts; in-control ARL 500.